# Phosphoinositide 3-kinase δ regulates membrane fission of Golgi carriers for selective cytokine secretion

Pei Ching Low,[1] Ryo Misaki,[1] Kate Schroder,[1] Amanda C. Stanley,[1] Matthew J. Sweet,[1] Rohan D. Teasdale,[1] Bart Vanhaesebroeck,[4] Frédéric A. Meunier,[2,3] Tomohiko Taguchi,[1] and Jennifer L. Stow[1]

[1]Institute for Molecular Bioscience, [2]Queensland Brain Institute, and [3]School of Biomedical Science, The University of Queensland, Brisbane, Queensland 4072, Australia
[4]Centre for Cell Signalling, Institute of Cancer, Queen Mary University of London, London EC1M 6BQ, England, UK

Phosphoinositide 3-kinase (PI3K) p110 isoforms are membrane lipid kinases classically involved in signal transduction. Lipopolysaccharide (LPS)-activated macrophages constitutively and abundantly secrete proinflammatory cytokines including tumor necrosis factor-α (TNF). Loss of function of the p110δ isoform of PI3K using inhibitors, RNA-mediated knockdown, or genetic inactivation in mice abolishes TNF trafficking and secretion, trapping TNF in tubular carriers at the trans-Golgi network (TGN). Kinase-active p110δ localizes to the Golgi complex in LPS-activated macrophages, and TNF is loaded into p230-labeled tubules, which cannot undergo fission when p110δ is inactivated. Similar blocks in fission of these tubules and in TNF secretion result from inhibition of the guanosine triphosphatase dynamin 2. These findings demonstrate a new function for p110δ as part of the membrane fission machinery required at the TGN for the selective trafficking and secretion of cytokines in macrophages.

## Introduction

The constitutive trafficking and secretion of newly synthesized proteins in mammalian cells is a complex, multistep pathway that is regulated by many protein and lipid families (Mellman and Warren, 2000). Key steps in this pathway include the formation of pleiomorphic, membrane-bound carriers for the transport of newly synthesized cargo through the cell (Bard and Malhotra, 2006). The ability to track fluorescently tagged cargo by live-cell imaging has revealed much about the behavior of these carriers, but many aspects of protein transport in secretory pathways remain ill defined (Hirschberg et al., 1998; Polishchuk et al., 2000; Keller et al., 2001; De Matteis and Luini, 2008).

The abundant, constitutive secretion of proinflammatory cytokines in macrophages represents a biologically and clinically important secretory pathway. Some features of this pathway are paradigmatic for eukaryotic cell function, whereas others have emerged as elegant adaptations for macrophage-specific functions in innate immunity (Murray et al., 2005a; Stow et al., 2006). Activation of macrophages by lipopolysaccharide (LPS) or other toll-like receptor (TLR) ligands initiates the synthesis, trafficking, and secretion of proinflammatory cytokines (Gordon, 2007; Stow et al., 2009). TNF is one of the major early response inflammatory cytokines released by macrophages. Although TNF is an essential proponent of inflammation and immunity, its overabundant secretion from activated macrophages in chronic inflammatory diseases is highly detrimental in a clinical context (Beutler, 1999). Therefore, it is imperative to fully define and understand the regulators of TNF trafficking and secretion.

Newly synthesized transmembrane precursors of TNF are transported from the TGN to recycling endosomes from where TNF can be rapidly deployed to phagocytic cups or filopodia at the cell surface for cleavage and release (Murray et al., 2005a; Stow et al., 2009). LPS up-regulates the expression of specific membrane fusion proteins (Pagan et al., 2003; Murray et al., 2005b; Stow et al., 2006) and increases the budding of

Correspondence to Jennifer L. Stow: j.stow@imb.uq.edu.au

Abbreviations used in this paper: BMM, bone marrow–derived macrophage; Dyn2, dynamin 2; IL-6, interleukin-6; LPS, lipopolysaccharide; PE, R-phycoerythrin; PI3K, phosphoinositide 3-kinase; PtdIns(3,4,5)$P_3$, phosphatidylinositol-3,4,5-bisphosphate; PtdIns(4,5)$P_2$, phosphatidylinositol-4,5-bisphosphate; TACE, TNF-converting enzyme; TfnR, transferrin receptor; TLR, toll-like receptor; WT, wild type.



The Rockefeller University Press $30.00
J. Cell Biol. Vol. 190 No. 6 1053–1065
www.jcb.org/cgi/doi/10.1083/jcb.201001028

TGN-derived membrane carriers to facilitate TNF trafficking and secretion (Lock et al., 2005; Lieu et al., 2008). Thus, in macrophages, key features of constitutive secretion are tightly linked to cell activation, presumably through cell signaling pathways. How signaling and membrane trafficking are coordinated during macrophage activation is unclear, and thus, we sought to identify additional regulators involved in stimulus-coupled cytokine release.

Phosphoinositide 3-kinases (PI3Ks) are ubiquitous modulators of cellular membrane lipids for signaling and trafficking events. Members of the three mammalian PI3K classes (I–III), which differ in their molecular structures and substrate specificities, generate 3′-phosphorylated phosphoinositides on the cytoplasmic leaflet of membrane bilayers for diverse roles in signal transduction, cytoskeletal dynamics, and membrane trafficking (for reviews see Martin, 1998; Vanhaesebroeck et al., 2001; Di Paolo and De Camilli, 2006). The classical signal-transducing class I PI3Ks are heterodimers comprising four catalytic isoforms (p110α, p110β, p110δ, or p110γ) complexed to their membrane-targeting adaptors. These represent the only class of PI3Ks that can metabolize phosphatidylinositol-4,5-bisphosphate (PtdIns(4,5)$P_2$) to yield phosphatidylinositol-3,4,5-bisphosphate (PtdIns(3,4,5)$P_3$) in vivo, often in response to cell activation. PtdIns(3,4,5)$P_3$ plays a major role in delineating docking sites for a variety of protein effectors possessing the pleckstrin homology domains, including serine/threonine kinases, tyrosine kinases, nucleotide exchange factors, and GTPases, which control a diversity of cellular functions, exquisitely under PI3K regulation (Vanhaesebroeck and Waterfield, 1999; Deane and Fruman, 2004). Class I PI3Ks have not previously been implicated in regulation of constitutive secretion (Lindmo and Stenmark, 2006).

In this study, our experiments led us to examine a role for PI3K in TNF secretion in macrophages. Our findings show a new and unexpected function for one member of the class I PI3K subfamily in intracellular trafficking at the level of the TGN.

## Results

### The p110δ isoform of PI3K regulates constitutive secretion of TNF

As one approach to identifying molecular regulators of intracellular TNF trafficking, a screen of pharmacologic agents was performed in LPS-activated mouse macrophages. Results showed that treatment with either of the pan-PI3K inhibitors, wortmannin or LY294002, altered TNF secretion. In an earlier study, wortmannin added before LPS was found to increase the amount of TNF secreted from peritoneal macrophages (Park et al., 1997). Inhibitors in our experiments were added with LPS to modify subsequent trafficking, and under these conditions, wortmannin and LY294002 strikingly suppressed TNF secretion over a 6-h time course in RAW264.7 cells (Fig. 1 A). Titrated into culture supernatants, LY294002 reduced TNF secretion in a concentration-dependent manner, optimally at >25 µM (by ∼60−80%) over the time course (Fig. S1 A). The more potent wortmannin maximally reduced TNF secretion by up to 70% at low nanomolar concentrations (<250 nM) over 6 h, which is consistent with its relatively short half-life (Fig. S1 B; Vanhaesebroeck and Waterfield, 1999). At these concentrations, both drugs are known to inhibit most subtypes of PI3K, particularly the class I kinases (Fruman et al., 1998). Secondary testing using specific inhibitors to the different class I catalytic isoforms was performed (Fig. 1 B). LPS-stimulated TNF secretion was significantly reduced (by 60%) by 5 µM IC87114, at which concentration this inhibitor is highly selective for p110δ (Sadhu et al., 2003). The p110β-selective inhibitor TGX221 also affected TNF secretion at the highest concentration tested (500 nM), which can also inactivate p110δ (Jackson et al., 2005). In contrast, other p110 inhibitors had only marginal effects on TNF secretion. These results provided initial evidence that PI3K, specifically its p110δ isoform, is active in modulating the constitutive secretion of TNF.

The trafficking of TNF to the cell surface in LPS-activated macrophages can be assayed by sequential immunostaining of plasma membrane and intracellular pools of TNF (Pagan et al., 2003). LPS-activated macrophages incubated with a TNF-converting enzyme (TACE) inhibitor to block proteolytic release of TNF can be fixed and stained without permeabilization to detect surface-retained TNF (Fig. 1 C); subsequent permeabilization then allows for labeling of intracellular TNF, typically at the perinuclear Golgi complex (Fig. 1 C; Shurety et al., 2000). LY294002 treatment resulted in dramatically reduced surface staining of TNF, but TNF was still present inside the cells, detected as strong perinuclear Golgi staining (Fig. 1 C). To quantitate the effects of p110δ inhibition on the cell surface delivery of TNF, macrophages treated for 2 h with 5 µM IC87114 or pan-PI3K inhibitors (15 nM wortmannin or 25 µM LY294002) were subjected to similar staining procedures for flow cytometric analysis. All inhibitors caused a >60% reduction in staining intensity of surface TNF, relative to control cells, whereas staining of intracellular TNF was not significantly affected (Fig. 1 D and Fig. S2 A). Collectively, these data show that pan-PI3K or p110δ-selective pharmacologic inhibition blocks the surface delivery and secretion of TNF, without affecting its de novo synthesis. Moreover, inactivation of p110δ alone was as efficacious in blocking TNF surface delivery as pan-PI3K inhibition, suggesting that p110δ is the sole or predominant PI3K isoform active in this trafficking pathway.

### TNF trafficking is blocked by siRNA-mediated knockdown of p110δ and by its genetic inactivation in mice

To directly test the requirement for p110δ in transporting TNF to the cell surface, small interfering (si) RNA knockdown was used to silence p110δ expression in RAW264.7 macrophages. Three siRNAs were designed to target p110δ, and one (siRNA3) effectively reduced the levels of endogenous p110δ in total cell lysates by ∼90% (Fig. 2 A) and diminished immunostaining of p110δ in cells (Fig. 2 B). Immunostaining revealed a somewhat unexpected perinuclear concentration of p110δ staining in the Golgi region that correspondingly disappeared with the knockdown. In response to LPS, the amount of TNF secreted was shown to correlate inversely with the level of p110δ knockdown (Fig. 2 C). In siRNA3-treated cells, staining of TNF at the cell

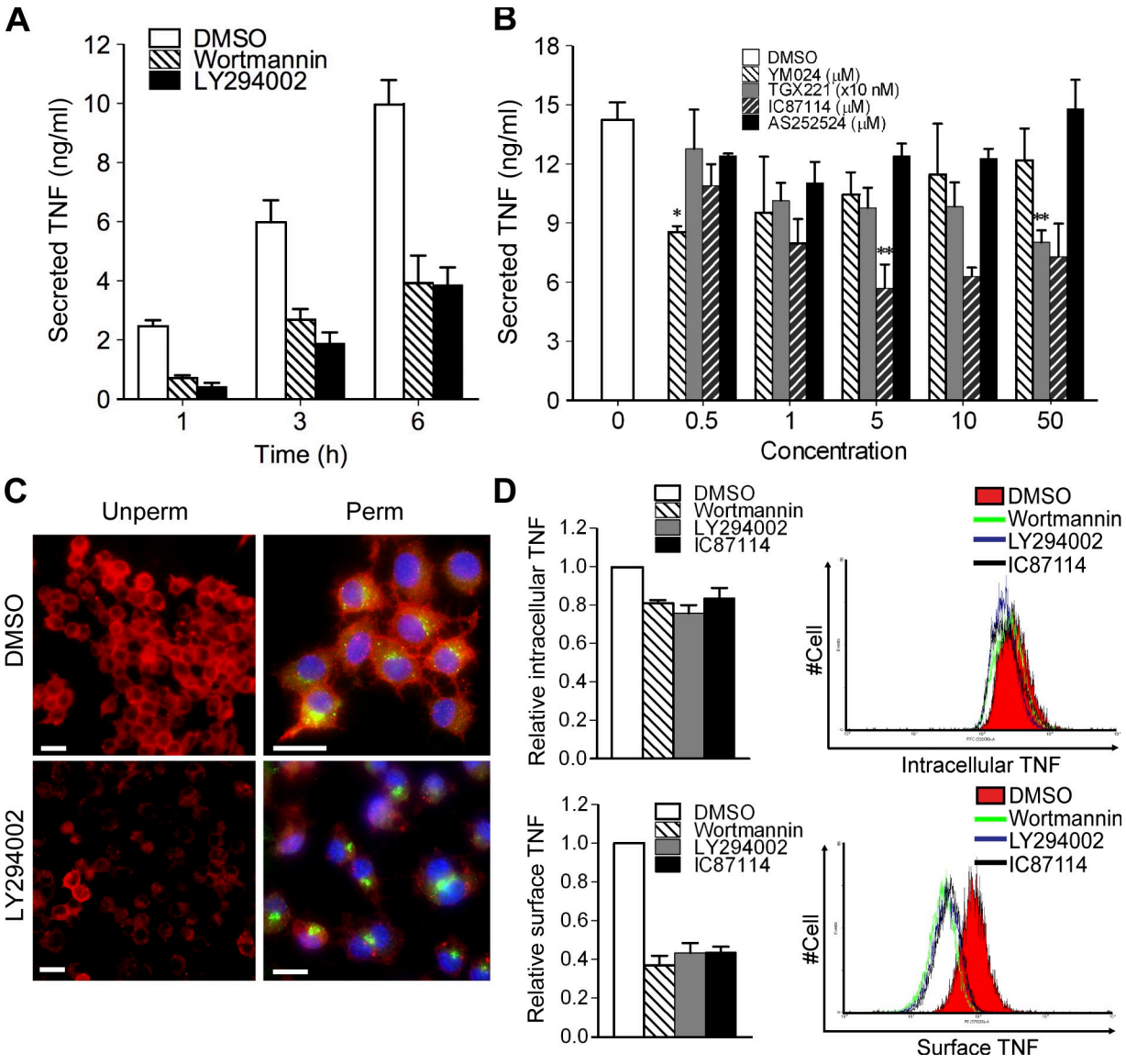


Figure 1. **PI3K inhibition and TNF secretion.** (A) RAW264.7 macrophages were stimulated with LPS in the presence of vehicle DMSO or either 15 nM wortmannin or 50 μM LY294002, and supernatants were sampled at the times indicated to measure TNF secretion by ELISA. (B) TNF secretion 2 h after LPS activation and treatment with p110-selective inhibitors (YM024 [p110α], TGX221 [p110β], IC87114 [p110δ], or AS252524 [p110γ]) at the concentrations indicated. The following indicate statistical significance at the lowest effective concentrations: ** (IC87114), P = 0.0025; ** (TGX221), P = 0.0073; * (YM024), P = 0.116. (C) Epifluorescence of RAW264.7 cells stimulated with LPS for 1 h in the presence of a TACE inhibitor, TAPI, to retain surface TNF. Cells treated with DMSO alone or with 50 μM LY294002. Immunostaining of surface TNF (red) on unpermeabilized (unperm) cells was followed by staining of intracellular TNF (green) after permeabilization (perm). DAPI (blue) labeling depicts nuclei. Bars, 10 μm. (D) Flow cytometric analysis of intracellular TNF (Alexa Fluor 488) and surface TNF (PE) staining in activated cells treated with DMSO, 15 nM wortmannin, 25 μM LY294002, or 5 μM IC87114 for 2 h. Mean fluorescence intensity of TNF staining in Alexa Fluor 488 or PE channel expressed as mean ratio ± SEM relative to DMSO. Corresponding representative overlay histograms are displayed. (A–D) All results are representative of three independent experiments. Error bars indicate mean ± SD.

surface was abolished (Fig. 2 B), and the level of secreted TNF in these cultures was decreased by >60% compared to controls or to cells transfected with siRNAs targeting other p110 isoforms (Fig. 2 C and not depicted). A rescue experiment was performed to rule out the possibility of siRNA off-target effects (Fig. 2 D and Fig. S3). Cells depleted of p110δ with siRNA3 were retransfected with an siRNA-resistant, wild-type (WT) plasmid (p110δ-WT). In cells now stained for exogenous p110δ, TNF staining was restored at the cell surface (Fig. 2 D and Fig. S3 A), indicating full rescue of TNF surface delivery. However, this rescue was not observed in cells transfected instead with an siRNA-resistant, kinase-dead plasmid (p110δ-kd; Fig. S3 B) nor by overexpression of a different PI3K (PI3KC2α; Fig. S3 C). These data thus provide evidence that the expression and kinase activity of p110δ is essential and nonredundant for effective cell surface delivery and secretion of TNF.

The in vivo function of p110δ can be studied in p110δ knockout mice (Clayton et al., 2002; Jou et al., 2002) and in mice lacking active p110δ, owing to a germline-inactivating knockin mutation (D910A) engineered in the p110δ kinase domain (Okkenhaug et al., 2002). Unlike the other class I PI3Ks, p110δ is predominantly and most highly expressed in leukocytes

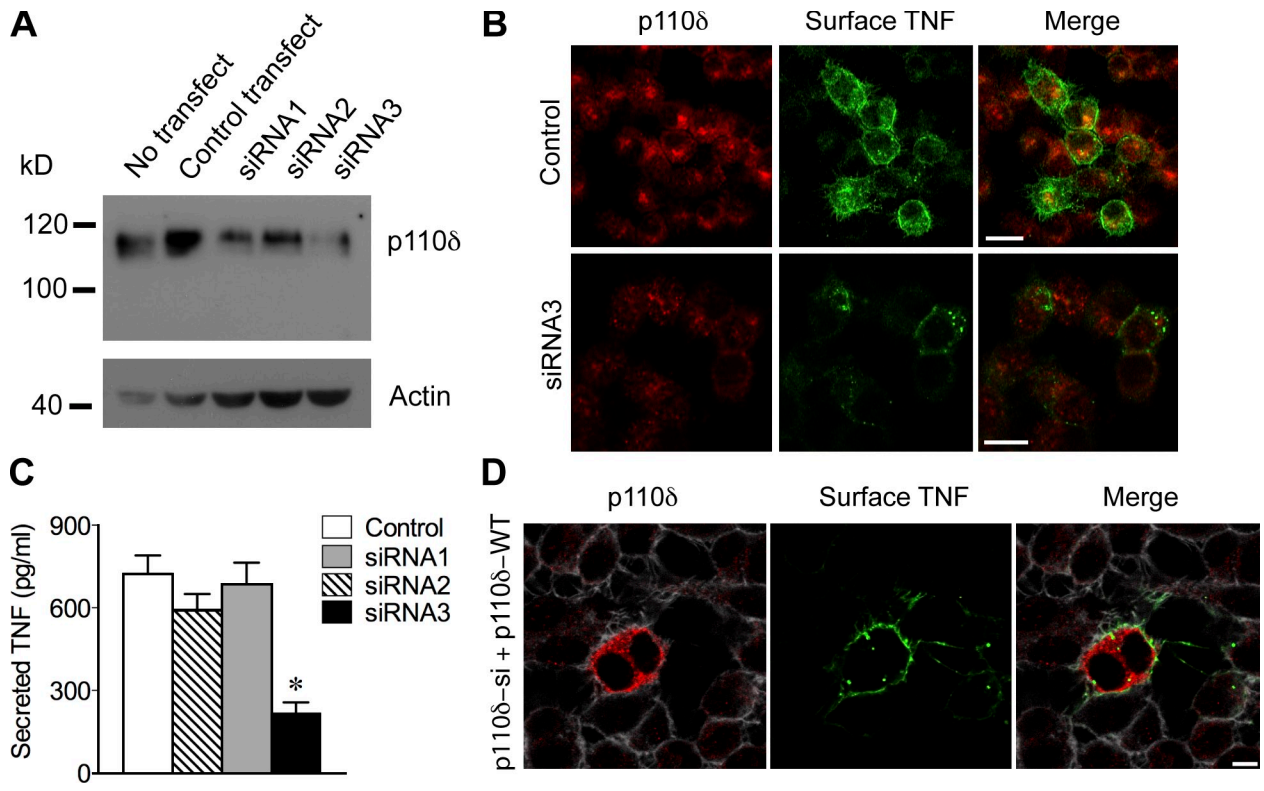


Figure 2. **siRNA knockdown of p110δ impairs TNF secretion.** (A) Levels of p110δ protein (~115 kD; loading control actin, ~40 kD) in cell lysates measured by Western blotting 48 h after transfection with specific siRNAs or controls. (B) Immunostaining of p110δ (red) and TNF (green) in cells after LPS activation in the presence of TAPI. siRNA3-transfected cells show reduced staining for both proteins. (C) Supernatants from mock-transfected (control) cells and cells transfected with p110δ-targeting siRNAs were used to measure TNF secretion by ELISA. Normalized to total protein, data are expressed as mean ± SEM from triplicate transfections. *, P = 0.0218. (D) Rescue of p110δ siRNA knockdown. Expression of siRNA-resistant WT p110δ (immunostained in red) in p110δ-si–transfected cells. Rescued cells show surface staining for TNF (green). LPS-activated cells were treated with TAPI, fixed, and immunostained. Phalloidin (white) was used to outline cells. Bars, 10 µm.

(Vanhaesebroeck et al., 1997; Okkenhaug and Vanhaesebroeck, 2003). Accordingly, homozygous mice with knockout or kinase-inactive mutant p110δ are viable but have a variety of immune cell signaling and functional defects (Vanhaesebroeck et al., 2005). The knockin transgenic strategy used to generate the $p110\delta^{D910A/D910A}$ mice provides an opportunity to investigate loss of p110δ kinase function without interfering with the molecular balance of other p110 isoforms and their associated adaptor subunits (Okkenhaug et al., 2002; Ali et al., 2004).

Therefore, we isolated bone marrow–derived macrophages (BMMs) from $p110\delta^{D910A/D910A}$ mice and WT littermates to study cytokine trafficking and secretion. Unstimulated WT and $p110\delta^{D910A/D910A}$ BMMs showed negligible TNF production or secretion (Fig. 3, A and C), as expected. In response to LPS stimulation, TNF secretion was detected in supernatants of both WT and $p110\delta^{D910A/D910A}$ BMMs by 2 h, and its secretion was maintained at high levels from 4–10 h only in WT cultures (Fig. 3 A). In contrast, TNF secretion from $p110\delta^{D910A/D910A}$ BMMs was severely reduced by 70–80% throughout the time course. This closely recapitulated the effects of IC87114 on LPS-stimulated secretion of TNF from RAW264.7 macrophages (Fig. 1 B). We also tested the ability of $p110\delta^{D910A/D910A}$ BMMs to effectively secrete cytokines other than TNF. Interleukin-6 (IL-6) is another proinflammatory cytokine whose biosynthetic trafficking pathway partially overlaps with that of TNF in RAW264.7 cells (Manderson et al., 2007). Upon LPS activation, both WT and $p110\delta^{D910A/D910A}$ BMMs produce IL-6, which was secreted alongside TNF (Fig. 3 B). Activated $p110\delta^{D910A/D910A}$ BMMs secreted IL-6 at levels similar to WT cells, which is consistent with only a modest impact of p110δ inactivation on secretion of this cytokine. Therefore, loss of p110δ activity selectively inhibits the trafficking and secretion of TNF but not IL-6 in BMMs. Although IL-6 secretion is not regulated by p110δ, it could nevertheless be reduced in RAW264.7 cells treated with LY294002 or wortmannin (Fig. S1, C and D, respectively), suggesting that other PI3K isoforms might be involved.

To confirm whether the observed reduction in TNF secretion from $p110\delta^{D910A/D910A}$ BMMs reflects a block in intracellular trafficking, cells were activated in the presence of the TACE inhibitor and stained for TNF for flow cytometric analysis. $p110\delta^{D910A/D910A}$ BMMs exhibited >80% lower surface TNF staining intensity than WT cells (Fig. 3 C and Fig. S2 B) despite similar levels of intracellular TNF. When individual BMMs were visualized by confocal microscopy, surface TNF staining on $p110\delta^{D910A/D910A}$ cells was minimal or absent, whereas intracellular TNF staining was still conspicuous (Fig. 3 D) and colocalized with GM130 at the Golgi complex (Fig. 3 E). Thus, these findings clearly show that $p110\delta^{D910A/D910A}$ BMMs still produce TNF but are defective in secreting it. This confirms

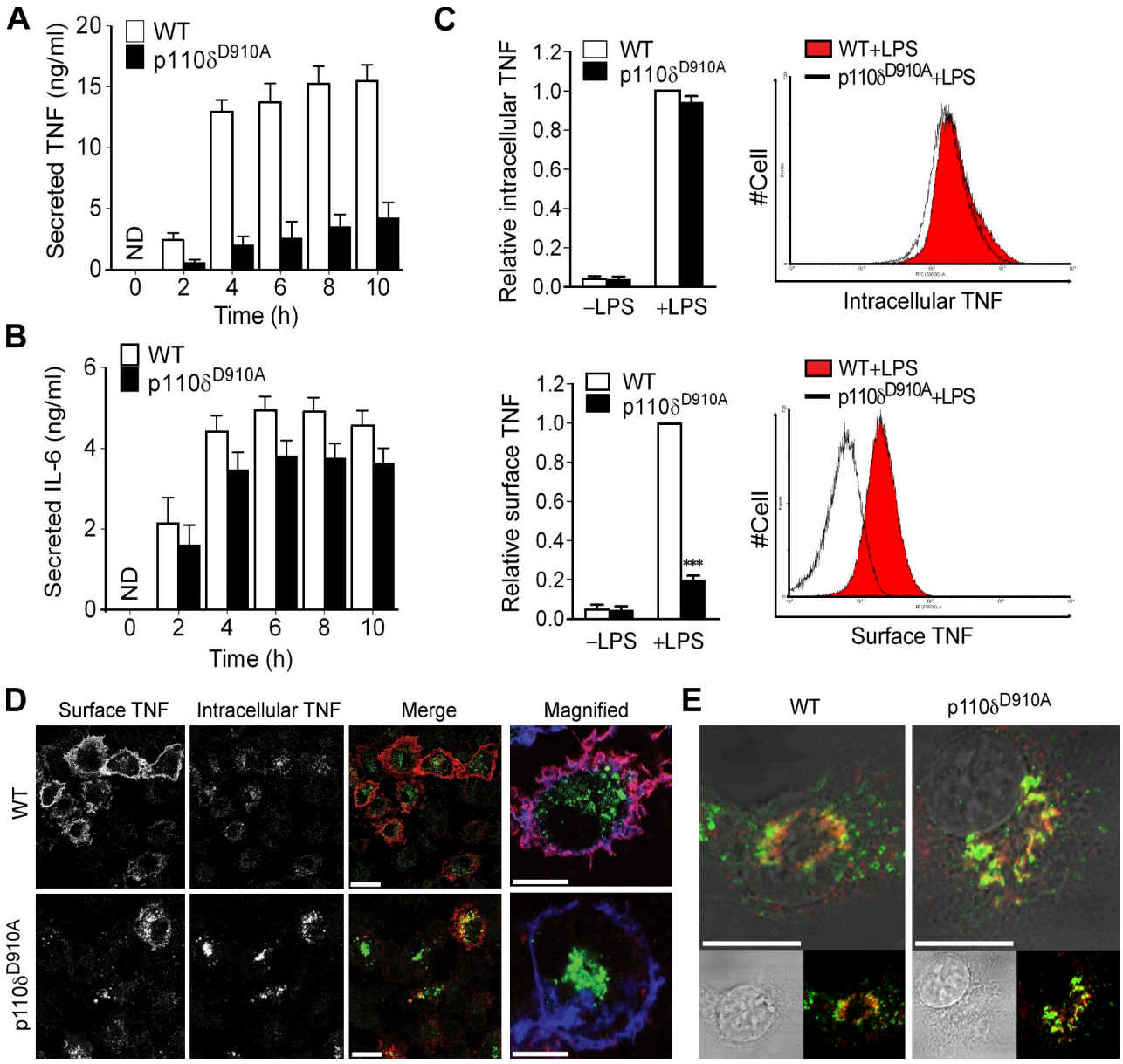


Figure 3. **Impaired trafficking and secretion of TNF in macrophages from genetically inactivated p110δ mice.** (A and B) Supernatants from LPS-stimulated WT and p110δ$^{D910A/D910A}$ BMM cultures were collected every 2 h over a 10-h time course for ELISA measurements of secreted TNF (A) and IL-6 (B). Results indicate mean ± SEM from three littermates of each genotype. ND, not detected. (C) Flow cytometric analysis of intracellular and surface TNF staining in WT and p110δ$^{D910A/D910A}$ BMMs treated with LPS and TAPI for 2 h. Mean fluorescence intensity in each TNF channel expressed as mean ratio ± SEM relative to LPS-stimulated WT from three independent experiments. ***, $P < 0.001$. Representative overlay histograms are shown for LPS-stimulated WT and p110δ$^{D910A/D910A}$ BMMs. (D and E) Confocal analysis of TNF staining in activated WT and p110δ$^{D910A/D910A}$ BMMs in the presence (D) or absence (E) of TAPI for 2 h. (D) Surface (red) and intracellular (green) TNF staining. Magnified images in D show BMMs costained with phalloidin (blue) to depict surface actin. (E) Intracellular TNF (green) in BMMs costained with the Golgi marker GM130 (red). Differential interference contrast images are included to define cells. Bars, 10 μm.

in primary cells that inactivation of p110δ does not affect the synthesis of TNF, nor its accumulation in the Golgi complex, but that subsequent delivery to the cell surface for secretion is impaired.

### LPS-inducible Golgi localization of p110δ

We next examined the localization and possible site of action for p110δ in macrophages. The p110 subunits of PI3K in various cell types are typically present in the cytoplasm or associated with plasma- and endomembranes at sites of their activation. Immunostaining of p110δ in LPS-activated RAW264.7 macrophages produced diffuse cytoplasmic staining and also concentrated p110δ labeling over the perinuclear Golgi complex that was costained for GM130 (Fig. 4 A). Staining with available antibodies to other isoforms produced only diffuse cytoplasmic staining, as shown for p110γ (Fig. 4 A). This reveals a novel localization for p110δ.

A biochemical approach was then used to assess and characterize the association of p110δ with Golgi membranes. Stacked Golgi membranes fractionated from homogenates

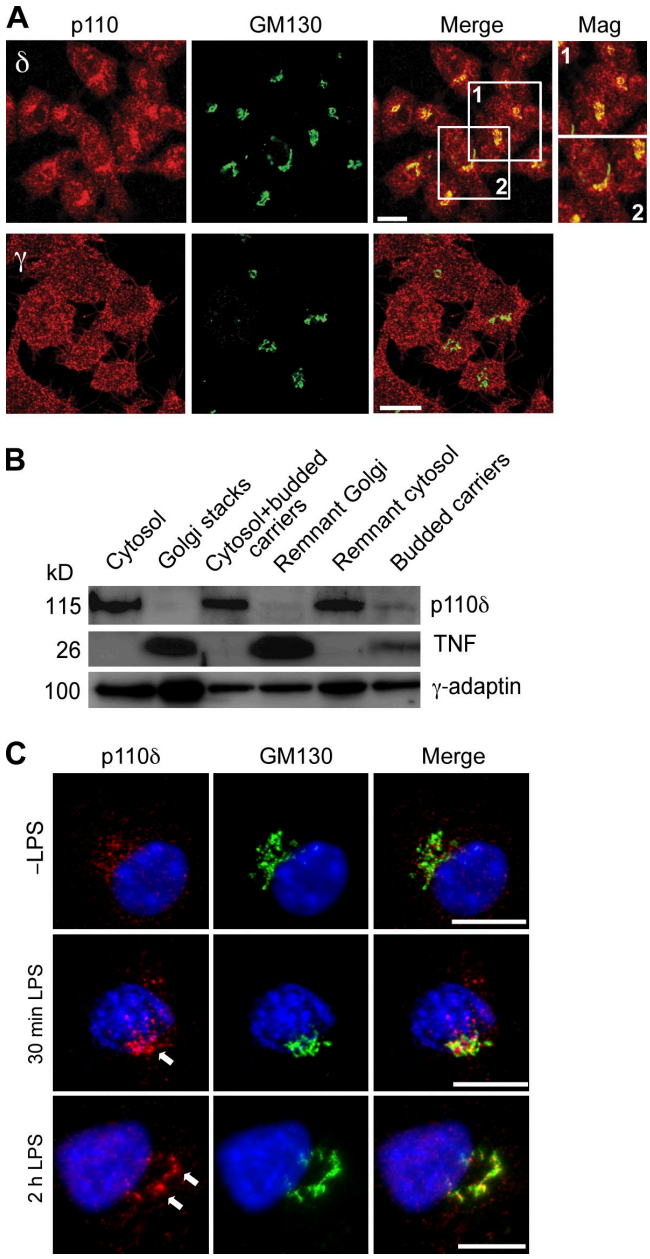


Figure 4. **Localization of p110δ on Golgi membranes.** (A) Confocal imaging reveals the diffuse cytoplasmic and Golgi immunostaining of p110δ (red) colocalized with GM130 (green; magnified) in RAW264.7 macrophages activated by LPS for 2 h. p110γ (red) gave mostly cytoplasmic immunostaining. (B) Stacked Golgi membranes prepared from activated RAW264.7 macrophages were incubated in vitro with cytosol and GTP-γS to generate budded carriers. The remnant Golgi membranes, budded carriers, and cytosol were collected by ultracentrifugations. Samples of these fractions were run on gels (25% of cytosol supernatants; whole membrane pellets) and immunoblotted for p110δ and γ-adaptin as a peripheral protein marker of TGN-derived budded carriers and TNF as cargo. (C) Coverslip-adherent RAW264.7 macrophages were stimulated with LPS over an acute time course. Immunostaining for p110δ (red) and GM130 (green) was performed at times 0, 30 min, and 2 h on ripped-open cells that exposed intact Golgi membranes. At least 20 cells were analyzed per three independent experiments. Arrows highlight colocalization of p110δ with GM130. DAPI (blue) labeling depicts nuclei. Bars, 10 µm.

of LPS-activated RAW264.7 cells contain TNF precursors as cargo; moreover, this TNF cargo can be recovered in a subset of carriers budded from the Golgi membranes after incubation in vitro with GTP-γS (Murray et al., 2005b; Manderson et al., 2007). In this study, a similar preparation was performed, and blotting revealed that p110δ was recovered mainly in the cytosol. p110δ was not detected as a resident protein on newly isolated or remnant Golgi membranes after budding; however, p110δ was recruited to membranes of budded carriers (Fig. 4 B). This carrier fraction also contained TNF as cargo. The adaptor protein γ-adaptin, which is also recruited from cytosol to carrier membranes, was blotted as a control to demonstrate carrier budding. These results confirm the transient association of p110δ with Golgi-derived membranes and further posit carrier membranes as a possible site of action for p110δ.

To further demonstrate an in situ recruitment of p110δ to Golgi membranes in response to acute LPS activation, we performed immunostaining of p110δ on perforated RAW264.7 macrophages from which the cytosol was depleted, leaving behind attached organelles (Wylie et al., 1999). The retention of nuclei and perinuclear Golgi complexes in cell remnants is shown by DAPI and GM130 labeling, respectively (Fig. 4 C). In unstimulated cells, some immunostained p110δ remained associated with Golgi after cell disruption. LPS activation of cells before disruption revealed markedly stronger staining of p110δ on the Golgi as early as 30 min and at 2 h as shown (Fig. 4 C, Fig. S4, and Video 1), which is consistent with recruitment of the kinase to these membranes. Strikingly, the timing of this LPS-inducible recruitment of p110δ correlates with the trafficking of a Golgi pool of newly synthesized TNF (Shurety et al., 2000) and with up-regulation of other known machinery needed for this trafficking (Murray et al., 2005a).

### TNF accumulates in Golgi-derived tubular carriers after PI3K inactivation

Newly synthesized TNF transported out of the Golgi complex moves to recycling endosomes before its final delivery to the cell surface (Murray et al., 2005a; Braun et al., 2007; Manderson et al., 2007). Our results to this point suggested that p110δ may be acting at the Golgi before the delivery of TNF to recycling endosomes. To further substantiate the requirement of PI3K activity in Golgi export of TNF to recycling endosomes, cells that had accumulated intracellular TNF during PI3K inhibition were colabeled with either transferrin receptor (TfnR) as a recycling endosomal marker or with GM130. In control cells, TNF and TfnR staining overlapped in some peripheral recycling endosomes (Fig. 5 A). However, after PI3K inhibition, little or no TNF was observed in these TfnR-labeled structures, whereas TNF was still broadly colocalized with GM130 at the Golgi complex. This confirms that PI3K inhibition blocks transport of TNF before it is delivered to recycling endosomes, precisely at its point of exit from the TGN. Upon close examination of fixed macrophages treated with LY294002 (Fig. 5, A and B) or IC87114 (not depicted), we noted the de novo appearance of multiple TNF-stained tubules emanating from Golgi complexes. These tubules were reminiscent of tubular extensions of the TGN seen in live cells (Polishchuk et al., 2000; De Matteis and Luini, 2008), and they specifically resembled

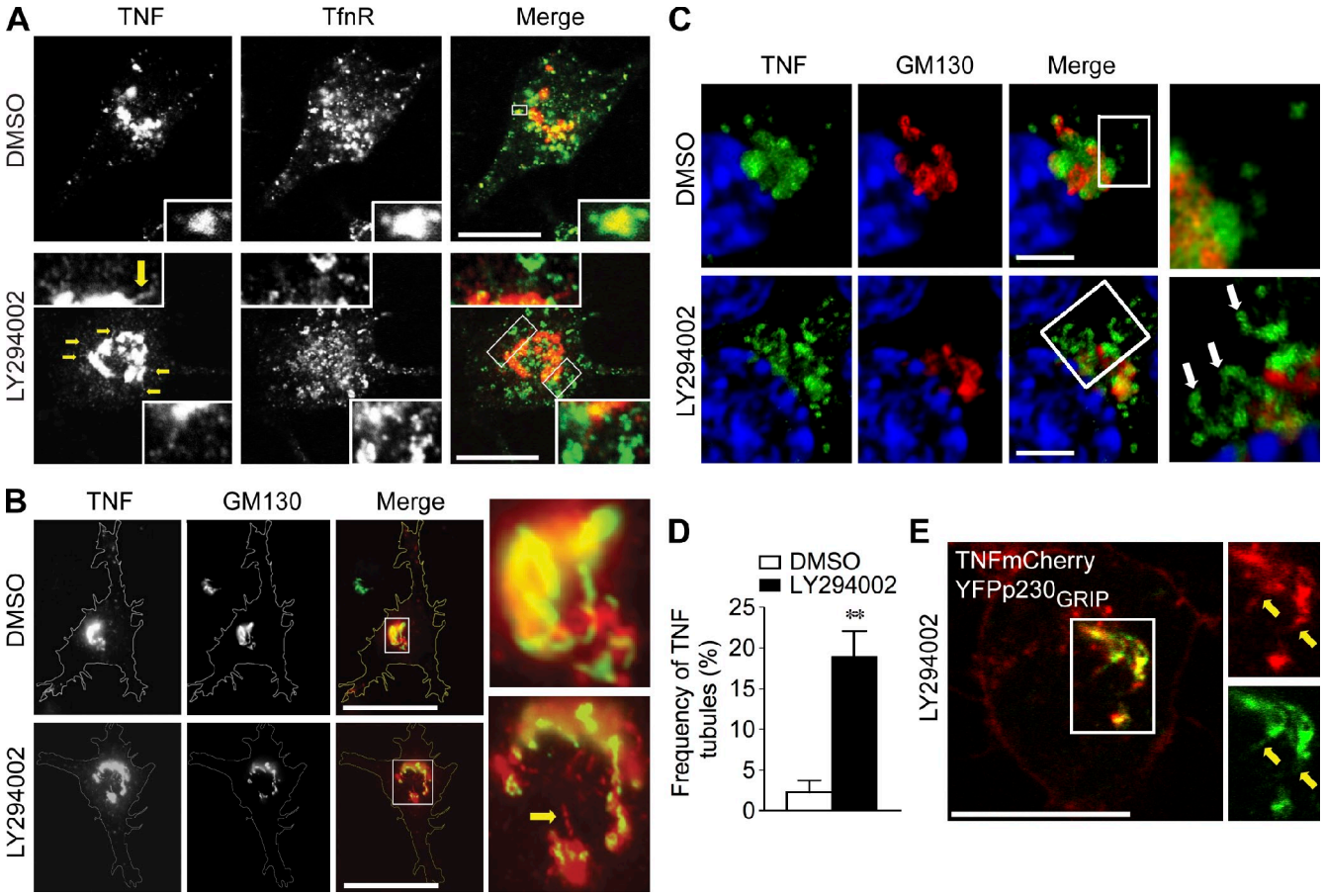


Figure 5. **Site of action for PI3K in TNF secretory pathway.** (A–C) LPS-activated RAW264.7 macrophages were incubated with DMSO or 50 µM LY294002 for 2 h, fixed, and immunostained for TNF (red) and, in green, either TfnR (A) or GM130 (B and C). Arrows in A point to multiple TNF-labeled tubules extending from the Golgi complex, and the arrow in B indicates one of these tubules labeled for TNF but not GM130. (C) 3D tomographic reconstructions of confocal z sections (0.48 µm) show multiple discrete TNF-positive tubules (arrows) after treatment with LY294002. DAPI (blue) labeling depicts nuclei. (D) TNF tubules were counted in cells from five fields (40–50 cells/field). Error bars indicate mean ± SEM. **, P = 0.0077. (E) RAW264.7 macrophages were transiently transfected with YFP-p230$_{GRIP}$ (green) and TNF-mCherry (red) for 2 h and treated with 50 µM LY294002 for 1 h before fixation for confocal microscopy. Arrows indicate two tubules (~3 and 13 µm in length). (A–C and E) Regions of colocalization or interest are indicated by boxes and are magnified in insets. Bars: (A, B, and E) 20 µm; (C) 10 µm.

the TNF-carrying tubular carriers we have previously reported (Lock et al., 2005; Lieu et al., 2008). Immunostaining confirmed the presence of TNF in these tubules and appropriately, the Golgi-resident protein GM130 was detected in the source Golgi complex but not in the tubules themselves (Fig. 5, B and C). Such tubular carriers are typically highly dynamic and therefore seen most readily in live cells (Lock et al., 2005). Their appearance in fixed macrophages after PI3K inhibition suggested enhanced activity or stability. Counting confirmed a marked >85% increase in TNF-stained, Golgi-associated tubules after incubation with pan-PI3K inhibitors (Fig. 5 D).

Proteins in the GRIP-golgin subfamily bind to and delineate distinct subdomains of the TGN and tubular carriers arising therefrom (Munro and Nichols, 1999; Gleeson et al., 2004). The tubules responsible for transporting TNF as cargo are specifically demarked by the GRIP-golgin p230 (also known as golgin-245 or t–golgin-1) and can be labeled by expression of the YFP-tagged, membrane-binding GRIP domain of p230 (YFP-p230$_{GRIP}$; Gleeson et al., 2004; Lock et al., 2005). Cotransfection of this YFP-p230$_{GRIP}$ and TNF-mCherry in activated RAW264.7 macrophages treated with LY294002 revealed tubules bearing both p230 and TNF labels (Fig. 5 E), indicating that the tubules seen under PI3K inhibition are bona fide TGN-derived tubular carriers for TNF.

### Inactivation of p110δ blocks fission of TGN tubular carriers in live macrophages

Our findings increasingly pointed to a novel role for p110δ at the level of TGN-derived exocytic tubular carriers. TGN carrier formation was then examined by high resolution, real-time imaging in live, activated RAW264.7 macrophages coexpressing YFP-p230$_{GRIP}$ and TNF-mCherry. YFP-p230$_{GRIP}$ tubules loaded with boluses of TNF-mCherry cargo were recorded emerging from the Golgi complex, often extending (up to ~7 µm) and rapidly (within 5.5 s) undergoing fission to release one or more boluses of TNF-mCherry (Fig. 6 A and Video 2).

When macrophages were activated in the presence of wortmannin (Fig. 6 B and Video 3) or IC87114 (Fig. 6 C and Video 4), YFP-p230$_{GRIP}$ tubules loaded with TNF-mCherry cargo were also observed, confirming patent cargo loading and formation of tubular carriers. However, inhibitor treatment

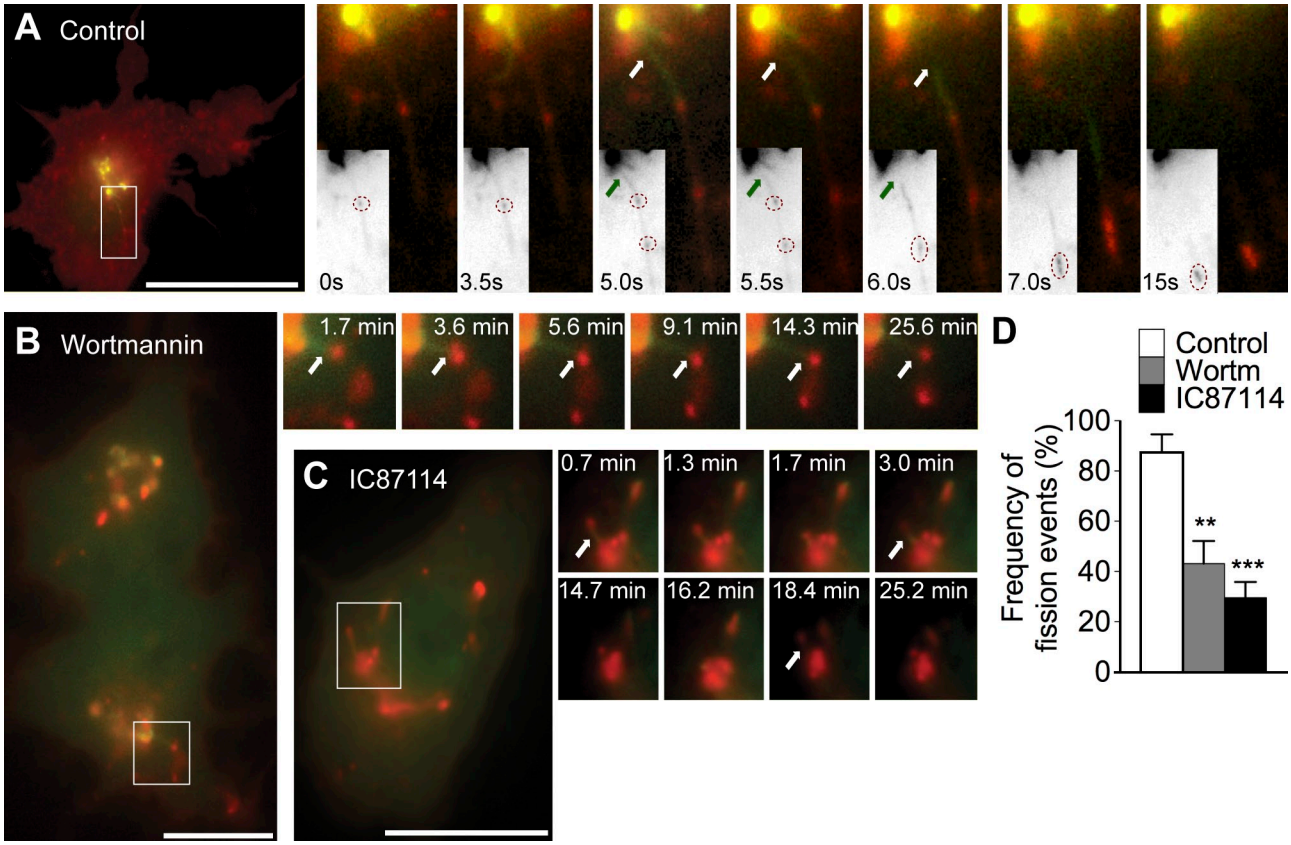


Figure 6. **p110δ regulates fission of TGN-derived, TNF-containing tubular carriers.** (A–C) RAW264.7 macrophages coexpressing YFP-p230$_{GRIP}$ (green) and TNF-mCherry (red) were treated with LPS only (A; control), LPS and 15 nM wortmannin (B), or LPS and 5 µM IC87114 (C) for at least 30 min before live cell imaging. (A) Selected stills from Video 2 depict tubular carriers labeled for YFP-p230$_{GRIP}$ emerging from the TGN and rapidly undergoing fission (white and green arrows) to release boluses of TNF-mCherry as cargo (dotted circles in grayscale insets). (B and C) Stills from Videos 3 and 4, respectively, also show YFP-p230$_{GRIP}$ tubules loaded with TNF-mCherry that were formed but cannot undergo fission. (D) Counting of fission events in TNF-mCherry–loaded YFP-p230$_{GRIP}$ tubules in live cells treated with LPS only (control), LPS and wortmannin (wortm), or LPS and IC87114 (IC87114). 30–40 cells were analyzed over eight transfections for each treatment. Error bars indicate mean ± SEM. **, P = 0.0022; ***, P < 0.0001. Regions of colocalization or interest are indicated by boxes and are magnified in insets. Bars, 20 µm.

resulted in tubules that remained remarkably inactive after forming and did not release TNF-mCherry, even over prolonged periods of recorded time (≥30 min). These tubules were able to extend (to ∼5–8 µm) and retract normally during observation periods, showing that their movement by itself was unaffected, but they remained atypically attached to the TGN, denoting fission as the likely defective step. Quantification confirmed that the frequency of fission events in live cells was over twofold lower in cells treated with wortmannin (87.59 ± 7.01% vs. 43.06 ± 9.08%; Fig. 6 D) or LY294002 (not depicted) and at least threefold lower (87.59 ± 7.01% vs. 29.50 ± 6.30%) in cells treated with IC87114 (Fig. 6 D) compared with controls. Thus, in live macrophages, inactivation of p110δ results in newly synthesized TNF that is still correctly loaded into p230 tubular carriers but cannot exit the TGN because of an apparent block in tubule fission.

The kinase activity of p110δ on Golgi membranes would produce its product PtdIns(3,4,5)$P_3$ at the same site. Accordingly, using a PtdIns(3,4,5)$P_3$-specific antibody, we were able to detect some PtdIns(3,4,5)$P_3$ upon LPS activation that colocalized with newly synthesized TNF at the Golgi (Fig. 7 A), and moreover, this staining disappeared from the membranes and from attached tubules containing TNF (Fig. 7 B, arrow) after treatment with IC87114. Thus, these data point to a pool of LPS-recruited active p110δ at the Golgi, congruent with the need to export newly synthesized TNF.

To further define how tubular fission is disrupted by inactivation of p110δ, we turned to other proteins known to induce membrane fission of Golgi-derived carriers. Such molecules include dynamin 2 (Dyn2), a large GTPase implicated in fission of TGN tubules transporting biosynthetic cargo (Jones et al., 1998; Cao et al., 2000; Kreitzer et al., 2000). Dyn2 also reportedly colocalizes with p230 at the TGN (Yang et al., 2001). When Dyn2 was overexpressed in activated macrophages, it broadly colocalized with YFP-p230$_{GRIP}$ on the TGN in addition to giving finely punctate, cytoplasmic immunostaining (Fig. 7 C). Treatment with IC87114 to inactivate p110δ dramatically diminished Dyn2 staining at the TGN in most cells (Fig. 7 C). Image analysis of TGN to cytoplasmic pixel intensities confirmed this loss of Dyn2 at the TGN (Fig. 7 D). This result confirms the dynamic recruitment of Dyn2 to TGN membranes seen previously in other cells (Cao et al., 2000; Kreitzer et al., 2000) and newly implicates PI3Kδ in Dyn2 recruitment. We also tested the functional consequence of blocking Dyn2 in preliminary experiments using the dynamin GTPase inhibitor dynasore (Macia et al., 2006). Dynasore treatment effectively abrogated LPS-stimulated TNF secretion comparable to the reduction observed from p110δ$^{D910A/D910A}$ BMMs,

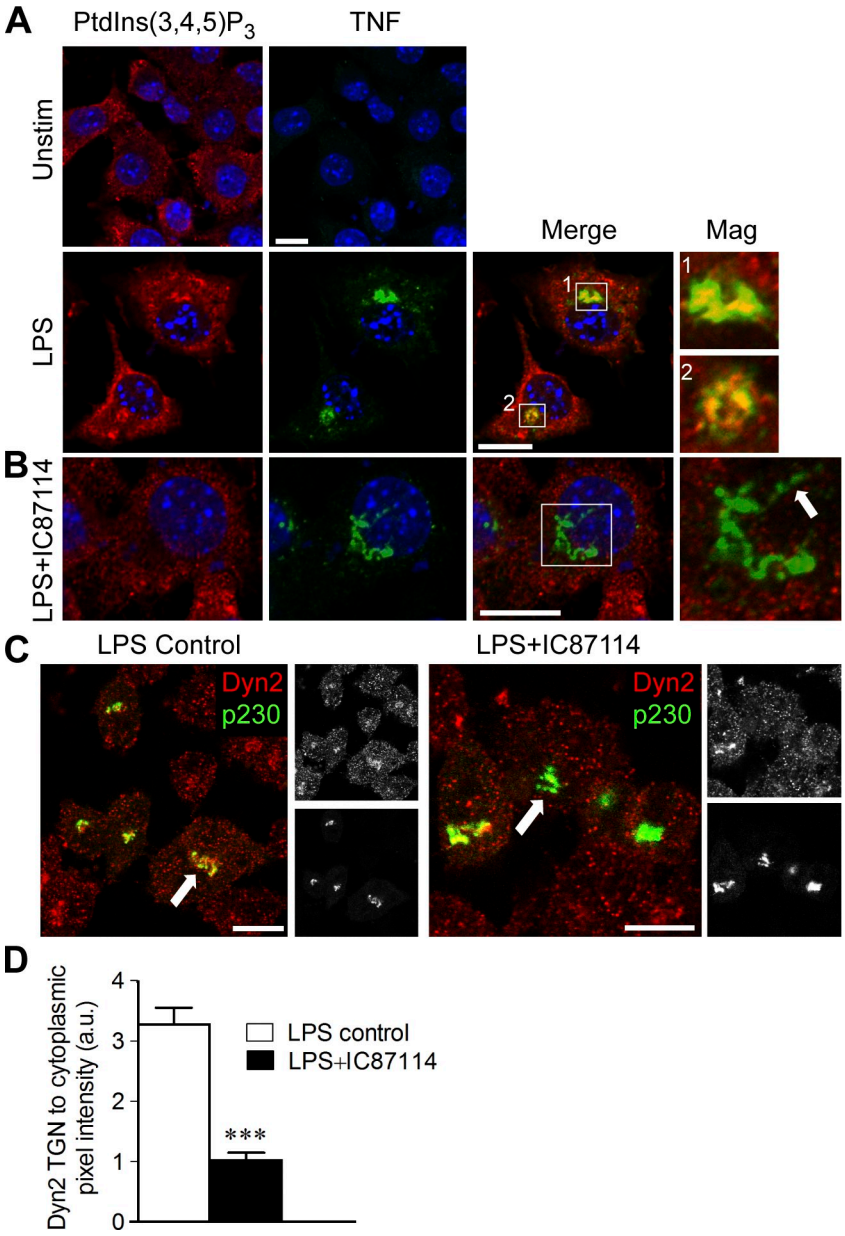


Figure 7. **Kinase activity of p110δ is required for TGN recruitment of Dyn2.** (A and B) Unstimulated RAW264.7 macrophages (unstim) and macrophages activated by LPS for 2 h in the absence or presence of 5 µM IC87114 were fixed for immunostaining for PtdIns(3,4,5)$P_3$ (red) and TNF (green). DAPI (blue) labeling depicts nuclei. Appearance of PtdIns(3,4,5)$P_3$ upon activation at perinuclear Golgi membranes colocalizing with TNF. This PtdIns(3,4,5)$P_3$ detection was selectively lost in the presence of IC87114. (C) RAW264.7 cells transiently transfected with YFP-p230$_{GRIP}$ (green) and untagged WT Dyn2 before activation by LPS for 2 h in the presence of DMSO (control) or 5 µM IC87114 were fixed for Dyn2 immunostaining (red). (B and C) Arrows indicate examples of colocalization of Dyn2 with p230 on TGN membranes that disappeared upon IC87114 treatment. (D) Activated cells coexpressing YFP-p230$_{GRIP}$ and Dyn2 treated with DMSO (control) or IC87114 as described in C were analyzed by image analysis to quantify relative distribution intensities of Dyn2 (TGN vs. cytoplasm). Data are represented as mean ratio ± SEM from 30 cells over three transfections. ***, $P < 0.0001$. Insets show magnified views of boxed regions. Bars, 10 µm.

producing only a small additive effect when used on these cells (Fig. S5 A). When dynasore was added to live RAW264.7 macrophages coexpressing YFP-p230$_{GRIP}$ and TNF-mCherry, dually labeled tubules were formed at the TGN but could not undergo fission (Fig. S5, B and C; and Video 5). Inhibition of Dyn2 thus appears to mimic the effect of inhibiting p110δ on p230/TNF tubule fission. These results now implicate Dyn2 as a necessary fission component for TNF trafficking in macrophages and a likely downstream effector of PI3Kδ.

## Discussion

The formation and fission of membrane tubules arising from the TGN as cargo carriers involves a complex array of proteins, many of them signaling proteins, such as the Gα and βγ subunits (Stow and Heimann, 1998; Jamora et al., 1999), PKD (Liljedahl et al., 2001; Hausser et al., 2005; Bard and Malhotra, 2006), and specific phospholipases (Chen et al., 1997; de Figueiredo et al., 1999; De Matteis and Luini, 2008; Yang et al., 2008). We now show in macrophages that an additional signaling protein from the PI3K family, PI3Kδ, is also part of this machinery. Our findings emerge from multiple approaches, including the use of pan-PI3K and isoform-specific pharmacologic inhibitors, as well as siRNA-mediated knockdown of the p110δ subunit in a macrophage cell line. These experiments consistently showed a marked, albeit incomplete, block in TNF secretion through selective retention of the cytokine within cells at the level of the Golgi complex. Genetic inactivation of p110δ in kinase-inactive mutant mice elaborated an even more profound block in the secretion of TNF from their BMMs. Our findings further demonstrate a novel location of kinase-active p110δ on Golgi membranes in activated macrophages. Live cell imaging provided the final mechanistic insights into the role of p110δ on these membranes in facilitating fission of TGN tubules carrying TNF. Collectively, these

experiments reveal a new site of action and function for PI3Kδ as a component of membrane fission machinery at the TGN.

Although the activities of PI3Ks are conventionally confined to signal transduction at the plasma membrane or in endocytic processes, prior studies have anticipated some PI3K involvement in exocytic carrier functions. Early biochemical in vitro studies using isolated Golgi membranes reported a Vps34-like PI3K activity associated with constitutive carrier budding on the TGN (Jones et al., 1993; Jones and Howell, 1997). Another study has also proposed a PI3K association with a human TGN protein, TGN46 (Hickinson et al., 1997). More recently, a wortmannin-insensitive class II PI3K, PI3KC2α, has been localized to TGN-derived clathrin-coated vesicles (Domin et al., 2000; Gaidarov et al., 2001) in addition to its known association with neurosecretory granules (Meunier et al., 2005). Interference with this kinase was shown to inhibit both clathrin-mediated endocytosis and TGN to lysosomal transport (Gaidarov et al., 2001). In this study, PI3KC2α could not rescue the TNF secretory defect induced upon knockdown of PI3Kδ (Fig. S3 C). So, it is plausible that different PI3K enzymes may in fact locate to the TGN, possibly to distinct subdomains, to selectively regulate transport out of the TGN. In this study, the identification of p110δ in regulating TGN export of TNF selectively in p230 tubules (Lock et al., 2005; Lieu et al., 2008) further suggests this level of TGN suborganization. Whether p110δ has an exclusive influence on p230 tubules remains to be determined. The soluble cytokine cargo IL-6, which can be loaded into multiple types of tubules to exit the TGN (Manderson et al., 2007), is only minimally affected in its secretion from p110δ-inactivated macrophages, yet its secretion is considerably down-regulated by pan-PI3K inhibitors (Fig. S1). Thus, p110δ is likely to have selective control over p230-mediated TGN export, whereas other PI3K isoforms may regulate the carriers for trafficking of other cytokines.

When p110δ is inactivated by pan and specific inhibitors and in fixed or live cells (Figs. 5 and 6), p230 tubules extend from the TGN preloaded with TNF as cargo, but they do not detach. This effectively traps TNF in tethered carriers and ultimately blocks secretion of this cytokine. All aspects of this trafficking phenotype are closely mimicked in our experiments by inhibiting the membrane fission GTPase Dyn2. These results first support the conclusion that p110δ functions at the level of tubular fission, and second, they newly implicate Dyn2 itself as part of the specific fission machinery for TNF/p230 tubules. Similar extension of cargo-loaded tubules that cannot detach result from mutation, inhibition, and/or knockdown of Dyn2 (Cao et al., 2000; Kreitzer et al., 2000; Jaiswal et al., 2009), PKD1-3, and Gβγ proteins (Liljedahl et al., 2001; Bard and Malhotra, 2006), and these deficits in tubule detachment have been reported as prima facie evidence to identify these molecules and others as part of the membrane fission machinery. Different TGN tubules appear to have disparate fission-inducing pathways in which distinct signaling proteins are positioned as upstream regulators or direct effectors of fission. PKD, for example, is a known regulator of PI4KIIIβ (Hausser et al., 2005) and thus of PtdIns(4)P- and PtdIns(4,5)$P_2$-mediated recruitment of fission factors (Godi et al., 1999, 2004); however, phospholipase D appears to play a more direct role in membrane fission of BARS-induced tubules (Yang et al., 2005, 2008). Along these lines, p110δ could act as an upstream regulator of Dyn2 either in its recruitment and/or activation via an LPS-dependent pool of PtdIns(3,4,5)$P_3$. Our localization data (Fig. 7 C) suggest that p110δ kinase activity is required for the TGN recruitment of Dyn2. Future extensive studies are now warranted to fully characterize this step in assembling this membrane fission machinery.

In macrophages, p110δ functions as a key part of an LPS-induced machinery that simultaneously up-regulates the specific carriers and molecules needed to transport the wave of newly synthesized cytokines destined for secretion. It has recently emerged that specific steps in constitutive trafficking pathways can be modulated by signaling to accommodate cargo volume changes (Pulvirenti et al., 2008). We now show that the involvement of p110δ, which also signals downstream of TLRs (Okkenhaug and Vanhaesebroeck, 2003), serves to directly link LPS cell activation with membrane trafficking capacity. Indeed, fine tuning of trafficking at the level of the TGN carriers and at the subsequent recycling endosome and cell surface help to ensure that macrophages elicit the temporally controlled sequence of pro- and antiinflammatory cytokines so critical for orchestrating an inflammatory response.

p110δ is mainly expressed in leukocytes, as demonstrated by the varying effects of p110δ inactivation on B lymphocytes, T lymphocytes, natural killer cells, and mast cells in the $p110\delta^{D910A/D910A}$ mice. Anomalies in cytokine release have been documented in several of these cell types. Mast cells derived from $p110\delta^{D910A/D910A}$ mice have reduced degranulation and secretion of TNF and IL-6, protecting them from anaphylactic allergic reactions (Ali et al., 2004). B lymphocytes from these mice have reduced TLR-mediated IL-6 and IL-10 secretion (Dil and Marshall, 2009). Most of these experiments concluded that p110δ inactivation and loss of signaling disrupts cytokine synthesis. Not so in natural killer cells from p110δ knockout mice (Kim et al., 2007), where it was noted that intracellular levels of cytokines were sustained even though there was reduced secretion. Our findings now show squarely that TLR signaling successfully initiates the synthesis of TNF and IL-6 in $p110\delta^{D910A/D910A}$ BMMs. The defect as pinpointed in RAW cells, in BMMs, and by live imaging is at the level of trafficking and TGN exit. In showing that p110δ functions selectively in the fission of some TGN tubular carriers, we can now explain why the secretion of only some cytokines is abrogated in different immune cell types from $p110\delta^{D910A/D910A}$ and p110δ knockout mice. It will now be important to catalog which cytokines are transported by different TGN tubules in various cell types. Our findings highlight the potential of p110δ inhibition as a means for selective abrogation of cytokine secretion in the treatment of chronic inflammatory diseases.

## Materials and methods

### Antibodies, plasmids, and inhibitors

Rabbit polyclonal (Merck) and rat monoclonal (Auspep) antibodies recognizing mouse TNF (Murray et al., 2005a) and monoclonal antibodies specific for GM130 (BD), Dyn2 (BD), and TfnR (Invitrogen) were used. A rabbit polyclonal antibody raised against a 20–amino acid C-terminal peptide of p110δ was sourced from Abcam (Vanhaesebroeck et al., 1997). Rabbit antibodies against the other p110 isoforms (p110α, p110β, and p110γ) were obtained from Cell Signaling Technology. A mouse monoclonal antibody specific for PtdIns(3,4,5)$P_3$ was obtained from Echelon (Papakonstanti et al., 2007).

Secondary antibodies used were R-phycoerythrin (PE)-conjugated monoclonal antibody to mouse TNF (BD; Murray et al., 2005a) and Cy3- or Alexa Fluor 488–conjugated anti–mouse, –rabbit, or –rat IgGs (all obtained from Jackson ImmunoResearch Laboratories, Inc.). cDNA plasmids used for live cell imaging encoding full-length TNF N-terminally tagged with mCherry (TNF-mCherry) or the GRIP domain of p230 C-terminally tagged with YFP (YFP-p230$_{GRIP}$) have all been previously described (Lock et al., 2005; Manderson et al., 2007; Lieu et al., 2008). Plasmids encoding untagged, full-length human WT p110δ or kinase-dead p110δ (R894P) have been described previously (Vanhaesebroeck et al., 1997). PI3KC2α-GFP was provided by J. Domin (Imperial College, London, England, UK). A plasmid encoding untagged, full-length WT Dyn2 was provided by M.A. McNiven (Mayo Clinic, Rochester, MN).

TAPI was purchased from EMD. Wortmannin and LY294002 were obtained from Sigma-Aldrich and Cell Signaling Technology, respectively. Small molecule p110-selective inhibitors YM024 (p110α), TGX-221 (p110β), and AS252424 (p110γ) were provided by S. Jackson (Australian Centre for Blood Diseases, Monash University, Melbourne, Victoria, Australia), and IC87114 (p110δ) was supplied by Symansis. Dynasore was obtained from Sigma-Aldrich. All inhibitors were reconstituted in DMSO (Sigma-Aldrich) with final concentration of DMSO in assays at 0.1% maximum.

**Cell culture, activation, and transfection**

The mouse RAW264.7 macrophage cell line was cultured in RPMI1640 (BioWhittaker; supplemented with 10% heat-inactivated Serum Supreme [Cambrex] and 1% L-glutamine [Invitrogen]) in humidified 5% $CO_2$/95% air atmosphere at 37°C as previously described (Shurety et al., 2000). For experiments, cells were activated by addition of 100 ng/ml LPS (from *Salmonella minnesota* Re595; Sigma-Aldrich), and in some experiments, TNF cleavage was blocked with 10 µM TAPI. For transient expression of cDNAs or siRNAs, cells at ∼30–50% confluence were transfected using Lipofectamine 2000 (Invitrogen) according to the manufacturer's instructions and as previously described (Manderson et al., 2007). Cells were typically used for experiments 2–6 h after transfection of cDNAs.

To silence mouse p110δ, cells were transfected with three different specific siRNAs (*Pik3cd* Stealth; numbered 1–3; Invitrogen), cultured for 24 h, retransfected under the same conditions, and cultured for another 24 h before LPS activation (2 h) in the absence or presence of TAPI. Because siRNA3 reproducibly gave the strongest knockdown (Fig. 2), it was used in all subsequent si/rescue experiments. Human p110δ (WT or kinase dead) plasmids are siRNA3 resistant based on a different targeted sequence, and these were separately transfected into p110δ-si–depleted cultures for 6 h.

**Preparation of mouse BMMs**

BMMs were derived by ex vivo differentiation of bone marrow progenitors extracted from femurs of at least 6- to 8-wk-old mice in accordance with the Australian animal ethics guidelines. BMMs were prepared from both p110δ$^{D910A/D910A}$ kinase-dead mutant mice (Okkenhaug et al., 2002), and WT littermates inbred on the C57BL/6 genetic background were kept under pathogen-free conditions. Bone marrow cells were pooled from equal numbers of age-matched mice in each experiment and cultured for 7 d in growth medium supplemented with CSF-1 (10,000 U/ml; provided by Novartis) before use, as previously described (Hume and Gordon, 1983).

**Assaying cytokine secretion**

To determine the levels of secreted TNF or IL-6, macrophages (RAW, 2 × $10^5$/ml; BMM, 5 × $10^5$/ml) were stimulated with LPS, and commercial ELISA kits (BD OptEIA; BD) or the Cytometric Bead Array system (BD) was used to quantify cytokine concentrations in samples according to the manufacturer's instructions. For assaying TNF secretion in the presence of wortmannin, LY294002, p110-selective inhibitors, or dynasore (each drug at the concentrations indicated in Figs. 1–7), DMSO (0.1% final) was added with LPS into the supernatant.

**Fluorescence microscopy, live cell imaging, and flow cytometry**

Immunofluorescence staining was performed as previously described (Pagan et al., 2003) on coverslip-adherent macrophages fixed for 1 h at room temperature in 4% paraformaldehyde. For some experiments (Fig. 4 C and Fig. S4), adherent macrophages were briefly air dried, and their exposed membranes ripped off by gentle application (30 s) and removal of partially damp filter paper (Millipore; Wylie et al., 1999). Remnant cytoskeletons, basal membranes, and organelles left adhering to the coverslip were used for immunostaining. Washes were performed in PBS with or without BSA for blocking. Where required, cells were permeabilized in 0.1% Triton X-100 for 5 min (or 0.5% saponin for 10 min; Fig. 7, A and B). Fixed cells were sequentially incubated with appropriate primary and secondary antibodies and, in some cases, with Alexa Fluor 633 phalloidin (Invitrogen) and DAPI (Invitrogen). Coverslips were mounted in 50% glycerol containing DABCO (1,4-dazabiccyclo-2,2,2-octaine; Sigma-Aldrich) or ProLong gold reagent (Invitrogen). Epifluorescence still images were taken with a 12-Mp differential contrast camera (DP71; Olympus) on an upright microscope (BX-51; Olympus) fitted for a 60× NA 1.35 or 100× NA 1.4 oil objective using the associated DPController software (version 2.1; Olympus). Confocal images were acquired on an inverted microscope (LSM510 META; Carl Zeiss, Inc.) with a 63× or 100× NA 1.4 oil objective and an inverted microscope (LSM710; Carl Zeiss, Inc.) with a 63× NA 1.4 or 100× NA 1.46 oil objective using the associated META (LSM510) or ZEN (LSM510/710) software. For z series, images were sequentially captured with 0.4–0.7-µm step intervals, analyzed, and reconstructed in 3D using LSM, ZEN, and Volocity software (version 3.7; PerkinElmer). All images saved or exported in TIFF files after acquisition were analyzed using ImageJ (version 1.41; National Institutes of Health) and Photoshop (version 9–12; Adobe).

For live cell experiments, RAW macrophages were cultured on glass-bottom 35-mm dishes (MatTek). Real-time epifluorescence imaging was performed on a 100× NA 1.4 microscope (IX81; Olympus) with a 12-bit 1,376 × 1,032–pixel high resolution camera with cells bathed in $CO_2$-independent medium (Invitrogen; Lock et al., 2005; Murray et al., 2005a; Manderson et al., 2007) containing LPS and a PI3K inhibitor or dynasore and kept at 37°C inside the microscope incubator. Time-resolved image acquisition was controlled using the associated CellR software (version 2.5; Olympus). Frame capture rates were 0.5 s–0.1 min, with total acquisition periods of 15 s–40 min. Individual channels were captured sequentially, with typical capture rates of 0.1–1 s for YFP and 0.08–0.4 s for mCherry. Videos 1–5 were analyzed, cropped (if required), constructed using CellR, ImageJ, and Volocity, and exported as QuickTime videos (Apple) with playback speeds of 3 frames/s.

For flow cytometry, cultured cells were harvested, pelleted, and resuspended sequentially in PBS, 2% paraformaldehyde (30 min), BSA buffers, and PE-conjugated rabbit anti-TNF antibody (1 h) to detect cell surface TNF. To subsequently detect intracellular TNF, cells were pelleted and resuspended in 0.1% Triton X-100 (5 min) followed by rat anti-TNF antibody (1 h) and Alexa Fluor 488 goat anti–rat IgG (30 min) with in-between blocking washes. All steps were performed at 4°C. Cells were finally subjected to flow cytometric analysis on an LSR II (BD) using the associated acquisition software (FACSDiva; BD). Data were analyzed using WinMDI software (version 2.8; J. Trotter, The Scripps Research Institute, La Jolla, CA). Cells were gated on forward scatter/side scatter characteristics and on unstained and nonspecific isotype antibody controls. Levels of TNF fluorescence in each channel were assessed on the basis of mean fluorescence intensity in arbitrary units. All isotype-matched antibodies were purchased from BD.

**Preparation of cell lysates, SDS-PAGE separation, and Western blotting**

Cells were washed with PBS, harvested, and lysed in 10 mM Tris, pH 7.4, containing 1 mM EDTA, 0.5% Triton X-100, and Complete protease inhibitors (Roche) by passaging through a series of successively smaller needles. Lysates were centrifuged for 10 min at 17,000 *g*, and supernatants were assayed for protein content (Bradford assay; Bio-Rad Laboratories) before SDS-PAGE protein separation and analysis by Western blotting as described previously (Shurety et al., 2000). A stacked Golgi membrane fraction and subsequent Golgi-derived budded carriers were prepared from RAW264.7 macrophages stimulated with LPS for 2 h by a previously described method (Heimann et al., 1999; Wylie et al., 2003). In brief, postnuclear supernatants of homogenized macrophages were separated by ultracentrifugation on a discontinuous sucrose gradient to produce a stacked Golgi fraction. Both cytosol and Golgi stacks were sampled for Western blotting. The Golgi membranes were incubated in HKM buffer (20 mM KCl, 2.5 mM Mg acetate, and 25 mM Hepes-KOH, pH 7.4) in the presence of 0.1 mM GTP-γS and cytosol for 30 min at 37°C to allow budding of carriers. Golgi membranes were recovered by centrifugation at 17,500 *g* for 10 min at 4°C. Budded carriers were recovered from the supernatant by discontinuous sucrose gradient centrifugation as described previously (Heimann et al., 1999). Samples of cytosol, budded carriers, and remnant Golgi were analyzed by Western blotting.

**Statistical analysis and significance**

Statistical analysis was performed by two-tailed Student's *t* test using Prism software (version 5; GraphPad Software, Inc.). $P < 0.05$ was considered significant.

**Online supplemental material**

Fig. S1 shows the effects of pan-PI3K inhibitors on LPS-stimulated cytokine secretion from RAW264.7 macrophages. Fig. S2 shows representative density plots from flow cytometric analysis of surface and intracellular TNF levels in RAW264.7 and BMMs. Fig. S3 shows rescue of p110δ expression and TNF trafficking in siRNA–knocked down RAW264.7 macrophages. Fig. S4 shows 3D profiles of p110δ localization at the Golgi membranes. Fig. S5 shows the effects of inhibiting GTPase Dyn2 on TNF secretion and tubular fission. Video 1 shows a 3D reconstruction demonstrating in situ association of p110δ with Golgi membranes. Video 2 shows a typically dynamic p230/TNF tubule undergoing fission at the TGN in a representative activated macrophage. Video 3 shows a p230/TNF tubule that has formed at the TGN but cannot undergo fission in representative activated macrophages treated with wortmannin. Video 4 shows a p230/TNF tubule that has formed at the TGN but cannot undergo fission in a representative activated macrophage treated with IC87114. Video 5 shows p230/TNF tubules that formed at the TGN but cannot undergo fission in a representative activated macrophage treated with dynasore. Online supplemental material is available at http://www.jcb.org/cgi/content/full/jcb.201001028/DC1.

We thank Tatiana Khromykh, Juliana Venturato, and Darren Brown for technical assistance and colleagues whom we have acknowledged for kindly providing reagents.

The work was funded by grants and fellowships (to J.L. Stow, F.A. Meunier, and R.D. Teasdale) from the National Health and Medical Research Council of Australia. Confocal microscopy was performed at the Australian Cancer Research Foundation (ACRF)/Institute for Molecular Bioscience Dynamic Imaging Facility, which was established with the support of the ACRF. B. Vanhaesebroeck is an advisor to Intellikine (San Diego, CA).

Submitted: 7 January 2010
Accepted: 20 August 2010

## References

Ali, K., A. Bilancio, M. Thomas, W. Pearce, A.M. Gilfillan, C. Tkaczyk, N. Kuehn, A. Gray, J. Giddings, E. Peskett, et al. 2004. Essential role for the p110delta phosphoinositide 3-kinase in the allergic response. *Nature.* 431:1007–1011. doi:10.1038/nature02991

Bard, F., and V. Malhotra. 2006. The formation of TGN-to-plasma-membrane transport carriers. *Annu. Rev. Cell Dev. Biol.* 22:439–455. doi:10.1146/annurev.cellbio.21.012704.133126

Beutler, B.A. 1999. The role of tumor necrosis factor in health and disease. *J. Rheumatol. Suppl.* 57:16–21.

Braun, V., C. Deschamps, G. Raposo, P. Benaroch, A. Benmerah, P. Chavrier, and F. Niedergang. 2007. AP-1 and ARF1 control endosomal dynamics at sites of FcR mediated phagocytosis. *Mol. Biol. Cell.* 18:4921–4931. doi:10.1091/mbc.E07-04-0392

Cao, H., H.M. Thompson, E.W. Krueger, and M.A. McNiven. 2000. Disruption of Golgi structure and function in mammalian cells expressing a mutant dynamin. *J. Cell Sci.* 113:1993–2002.

Chen, Y.G., A. Siddhanta, C.D. Austin, S.M. Hammond, T.C. Sung, M.A. Frohman, A.J. Morris, and D. Shields. 1997. Phospholipase D stimulates release of nascent secretory vesicles from the trans-Golgi network. *J. Cell Biol.* 138:495–504. doi:10.1083/jcb.138.3.495

Clayton, E., G. Bardi, S.E. Bell, D. Chantry, C.P. Downes, A. Gray, L.A. Humphries, D. Rawlings, H. Reynolds, E. Vigorito, and M. Turner. 2002. A crucial role for the p110delta subunit of phosphatidylinositol 3-kinase in B cell development and activation. *J. Exp. Med.* 196:753–763. doi:10.1084/jem.20020805

de Figueiredo, P., R.S. Polizotto, D. Drecktrah, and W.J. Brown. 1999. Membrane tubule-mediated reassembly and maintenance of the Golgi complex is disrupted by phospholipase A2 antagonists. *Mol. Biol. Cell.* 10:1763–1782.

De Matteis, M.A., and A. Luini. 2008. Exiting the Golgi complex. *Nat. Rev. Mol. Cell Biol.* 9:273–284. doi:10.1038/nrm2378

Deane, J.A., and D.A. Fruman. 2004. Phosphoinositide 3-kinase: diverse roles in immune cell activation. *Annu. Rev. Immunol.* 22:563–598. doi:10.1146/annurev.immunol.22.012703.104721

Di Paolo, G., and P. De Camilli. 2006. Phosphoinositides in cell regulation and membrane dynamics. *Nature.* 443:651–657. doi:10.1038/nature05185

Dil, N., and A.J. Marshall. 2009. Role of phosphoinositide 3-kinase p110 delta in TLR4- and TLR9-mediated B cell cytokine production and differentiation. *Mol. Immunol.* 46:1970–1978. doi:10.1016/j.molimm.2009.03.010

Domin, J., I. Gaidarov, M.E. Smith, J.H. Keen, and M.D. Waterfield. 2000. The class II phosphoinositide 3-kinase PI3K-C2alpha is concentrated in the trans-Golgi network and present in clathrin-coated vesicles. *J. Biol. Chem.* 275:11943–11950. doi:10.1074/jbc.275.16.11943

Fruman, D.A., R.E. Meyers, and L.C. Cantley. 1998. Phosphoinositide kinases. *Annu. Rev. Biochem.* 67:481–507. doi:10.1146/annurev.biochem.67.1.481

Gaidarov, I., M.E. Smith, J. Domin, and J.H. Keen. 2001. The class II phosphoinositide 3-kinase C2alpha is activated by clathrin and regulates clathrin-mediated membrane trafficking. *Mol. Cell.* 7:443–449. doi:10.1016/S1097-2765(01)00191-5

Gleeson, P.A., J.G. Lock, M.R. Luke, and J.L. Stow. 2004. Domains of the TGN: coats, tethers and G proteins. *Traffic.* 5:315–326. doi:10.1111/j.1398-9219.2004.00182.x

Godi, A., P. Pertile, R. Meyers, P. Marra, G. Di Tullio, C. Iurisci, A. Luini, D. Corda, and M.A. De Matteis. 1999. ARF mediates recruitment of PtdIns-4-OH kinase-beta and stimulates synthesis of PtdIns(4,5)P2 on the Golgi complex. *Nat. Cell Biol.* 1:280–287. doi:10.1038/12993

Godi, A., A. Di Campli, A. Konstantakopoulos, G. Di Tullio, D.R. Alessi, G.S. Kular, T. Daniele, P. Marra, J.M. Lucocq, and M.A. De Matteis. 2004. FAPPs control Golgi-to-cell-surface membrane traffic by binding to ARF and PtdIns(4)P. *Nat. Cell Biol.* 6:393–404. doi:10.1038/ncb1119

Gordon, S. 2007. The macrophage: past, present and future. *Eur. J. Immunol.* 37(Suppl 1):S9–S17. doi:10.1002/eji.200737638

Hausser, A., P. Storz, S. Märtens, G. Link, A. Toker, and K. Pfizenmaier. 2005. Protein kinase D regulates vesicular transport by phosphorylating and activating phosphatidylinositol-4 kinase IIIbeta at the Golgi complex. *Nat. Cell Biol.* 7:880–886. doi:10.1038/ncb1289

Heimann, K., J.M. Percival, R. Weinberger, P. Gunning, and J.L. Stow. 1999. Specific isoforms of actin-binding proteins on distinct populations of Golgi-derived vesicles. *J. Biol. Chem.* 274:10743–10750. doi:10.1074/jbc.274.16.10743

Hickinson, D.M., J.M. Lucocq, M.C. Towler, S. Clough, J. James, S.R. James, C.P. Downes, and S. Ponnambalam. 1997. Association of a phosphatidylinositol-specific 3-kinase with a human trans-Golgi network resident protein. *Curr. Biol.* 7:987–990. doi:10.1016/S0960-9822(06)00418-0

Hirschberg, K., C.M. Miller, J. Ellenberg, J.F. Presley, E.D. Siggia, R.D. Phair, and J. Lippincott-Schwartz. 1998. Kinetic analysis of secretory protein traffic and characterization of golgi to plasma membrane transport intermediates in living cells. *J. Cell Biol.* 143:1485–1503. doi:10.1083/jcb.143.6.1485

Hume, D.A., and S. Gordon. 1983. Optimal conditions for proliferation of bone marrow-derived mouse macrophages in culture: the roles of CSF-1, serum, Ca2+, and adherence. *J. Cell. Physiol.* 117:189–194. doi:10.1002/jcp.1041170209

Jackson, S.P., S.M. Schoenwaelder, I. Goncalves, W.S. Nesbitt, C.L. Yap, C.E. Wright, V. Kenche, K.E. Anderson, S.M. Dopheide, Y. Yuan, et al. 2005. PI 3-kinase p110beta: a new target for antithrombotic therapy. *Nat. Med.* 11:507–514. doi:10.1038/nm1232

Jaiswal, J.K., V.M. Rivera, and S.M. Simon. 2009. Exocytosis of post-Golgi vesicles is regulated by components of the endocytic machinery. *Cell.* 137:1308–1319. doi:10.1016/j.cell.2009.04.064

Jamora, C., N. Yamanouye, J. Van Lint, J. Laudenslager, J.R. Vandenheede, D.J. Faulkner, and V. Malhotra. 1999. Gbetagamma-mediated regulation of Golgi organization is through the direct activation of protein kinase D. *Cell.* 98:59–68. doi:10.1016/S0092-8674(00)80606-6

Jones, S.M., and K.E. Howell. 1997. Phosphatidylinositol 3-kinase is required for the formation of constitutive transport vesicles from the TGN. *J. Cell Biol.* 139:339–349. doi:10.1083/jcb.139.2.339

Jones, S.M., J.R. Crosby, J. Salamero, and K.E. Howell. 1993. A cytosolic complex of p62 and rab6 associates with TGN38/41 and is involved in budding of exocytic vesicles from the trans-Golgi network. *J. Cell Biol.* 122:775–788. doi:10.1083/jcb.122.4.775

Jones, S.M., K.E. Howell, J.R. Henley, H. Cao, and M.A. McNiven. 1998. Role of dynamin in the formation of transport vesicles from the trans-Golgi network. *Science.* 279:573–577. doi:10.1126/science.279.5350.573

Jou, S.T., N. Carpino, Y. Takahashi, R. Piekorz, J.R. Chao, N. Carpino, D. Wang, and J.N. Ihle. 2002. Essential, nonredundant role for the phosphoinositide 3-kinase p110delta in signaling by the B-cell receptor complex. *Mol. Cell. Biol.* 22:8580–8591. doi:10.1128/MCB.22.24.8580-8591.2002

Keller, P., D. Toomre, E. Díaz, J. White, and K. Simons. 2001. Multicolour imaging of post-Golgi sorting and trafficking in live cells. *Nat. Cell Biol.* 3:140–149. doi:10.1038/35055042

Kim, N., A. Saudemont, L. Webb, M. Camps, T. Ruckle, E. Hirsch, M. Turner, and F. Colucci. 2007. The p110delta catalytic isoform of PI3K is a key player in NK-cell development and cytokine secretion. *Blood.* 110:3202–3208. doi:10.1182/blood-2007-02-075366

Kreitzer, G., A. Marmorstein, P. Okamoto, R. Vallee, and E. Rodriguez-Boulan. 2000. Kinesin and dynamin are required for post-Golgi transport of a plasma-membrane protein. *Nat. Cell Biol.* 2:125–127. doi:10.1038/35000081

Lieu, Z.Z., J.G. Lock, L.A. Hammond, N.L. La Gruta, J.L. Stow, and P.A. Gleeson. 2008. A trans-Golgi network golgin is required for the regulated secretion of TNF in activated macrophages in vivo. *Proc. Natl. Acad. Sci. USA.* 105:3351–3356. doi:10.1073/pnas.0800137105

Liljedahl, M., Y. Maeda, A. Colanzi, I. Ayala, J. Van Lint, and V. Malhotra. 2001. Protein kinase D regulates the fission of cell surface destined transport carriers from the trans-Golgi network. *Cell.* 104:409–420. doi:10.1016/S0092-8674(01)00228-8

Lindmo, K., and H. Stenmark. 2006. Regulation of membrane traffic by phosphoinositide 3-kinases. *J. Cell Sci.* 119:605–614. doi:10.1242/jcs.02855

Lock, J.G., L.A. Hammond, F. Houghton, P.A. Gleeson, and J.L. Stow. 2005. E-cadherin transport from the trans-Golgi network in tubulovesicular carriers is selectively regulated by golgin-97. *Traffic.* 6:1142–1156. doi:10.1111/j.1600-0854.2005.00349.x

Macia, E., M. Ehrlich, R. Massol, E. Boucrot, C. Brunner, and T. Kirchhausen. 2006. Dynasore, a cell-permeable inhibitor of dynamin. *Dev. Cell.* 10:839–850. doi:10.1016/j.devcel.2006.04.002

Manderson, A.P., J.G. Kay, L.A. Hammond, D.L. Brown, and J.L. Stow. 2007. Subcompartments of the macrophage recycling endosome direct the differential secretion of IL-6 and TNFalpha. *J. Cell Biol.* 178:57–69. doi:10.1083/jcb.200612131

Martin, T.F. 1998. Phosphoinositide lipids as signaling molecules: common themes for signal transduction, cytoskeletal regulation, and membrane trafficking. *Annu. Rev. Cell Dev. Biol.* 14:231–264. doi:10.1146/annurev.cellbio.14.1.231

Mellman, I., and G. Warren. 2000. The road taken: past and future foundations of membrane traffic. *Cell.* 100:99–112. doi:10.1016/S0092-8674(00)81687-6

Meunier, F.A., S.L. Osborne, G.R. Hammond, F.T. Cooke, P.J. Parker, J. Domin, and G. Schiavo. 2005. Phosphatidylinositol 3-kinase C2alpha is essential for ATP-dependent priming of neurosecretory granule exocytosis. *Mol. Biol. Cell.* 16:4841–4851. doi:10.1091/mbc.E05-02-0171

Munro, S., and B.J. Nichols. 1999. The GRIP domain - a novel Golgi-targeting domain found in several coiled-coil proteins. *Curr. Biol.* 9:377–380. doi:10.1016/S0960-9822(99)80166-3

Murray, R.Z., J.G. Kay, D.G. Sangermani, and J.L. Stow. 2005a. A role for the phagosome in cytokine secretion. *Science.* 310:1492–1495. doi:10.1126/science.1120225

Murray, R.Z., F.G. Wylie, T. Khromykh, D.A. Hume, and J.L. Stow. 2005b. Syntaxin 6 and Vti1b form a novel SNARE complex, which is up-regulated in activated macrophages to facilitate exocytosis of tumor necrosis Factor-alpha. *J. Biol. Chem.* 280:10478–10483. doi:10.1074/jbc.M414420200

Okkenhaug, K., and B. Vanhaesebroeck. 2003. PI3K in lymphocyte development, differentiation and activation. *Nat. Rev. Immunol.* 3:317–330. doi:10.1038/nri1056

Okkenhaug, K., A. Bilancio, G. Farjot, H. Priddle, S. Sancho, E. Peskett, W. Pearce, S.E. Meek, A. Salpekar, M.D. Waterfield, et al. 2002. Impaired B and T cell antigen receptor signaling in p110delta PI 3-kinase mutant mice. *Science.* 297:1031–1034.

Pagan, J.K., F.G. Wylie, S. Joseph, C. Widberg, N.J. Bryant, D.E. James, and J.L. Stow. 2003. The t-SNARE syntaxin 4 is regulated during macrophage activation to function in membrane traffic and cytokine secretion. *Curr. Biol.* 13:156–160. doi:10.1016/S0960-9822(03)00006-X

Papakonstanti, E.A., A.J. Ridley, and B. Vanhaesebroeck. 2007. The p110delta isoform of PI 3-kinase negatively controls RhoA and PTEN. *EMBO J.* 26:3050–3061. doi:10.1038/sj.emboj.7601763

Park, Y.C., C.H. Lee, H.S. Kang, H.T. Chung, and H.D. Kim. 1997. Wortmannin, a specific inhibitor of phosphatidylinositol-3-kinase, enhances LPS-induced NO production from murine peritoneal macrophages. *Biochem. Biophys. Res. Commun.* 240:692–696. doi:10.1006/bbrc.1997.7722

Polishchuk, R.S., E.V. Polishchuk, P. Marra, S. Alberti, R. Buccione, A. Luini, and A.A. Mironov. 2000. Correlative light-electron microscopy reveals the tubular-saccular ultrastructure of carriers operating between Golgi apparatus and plasma membrane. *J. Cell Biol.* 148:45–58. doi:10.1083/jcb.148.1.45

Pulvirenti, T., M. Giannotta, M. Capestrano, M. Capitani, A. Pisanu, R.S. Polishchuk, E. San Pietro, G.V. Beznoussenko, A.A. Mironov, G. Turacchio, et al. 2008. A traffic-activated Golgi-based signalling circuit coordinates the secretory pathway. *Nat. Cell Biol.* 10:912–922. doi:10.1038/ncb1751

Sadhu, C., B. Masinovsky, K. Dick, C.G. Sowell, and D.E. Staunton. 2003. Essential role of phosphoinositide 3-kinase delta in neutrophil directional movement. *J. Immunol.* 170:2647–2654.

Shurety, W., A. Merino-Trigo, D. Brown, D.A. Hume, and J.L. Stow. 2000. Localization and post-Golgi trafficking of tumor necrosis factor-alpha in macrophages. *J. Interferon Cytokine Res.* 20:427–438. doi:10.1089/107999000312379

Stow, J.L., and K. Heimann. 1998. Vesicle budding on Golgi membranes: regulation by G proteins and myosin motors. *Biochim. Biophys. Acta.* 1404:161–171. doi:10.1016/S0167-4889(98)00055-X

Stow, J.L., A.P. Manderson, and R.Z. Murray. 2006. SNAREing immunity: the role of SNAREs in the immune system. *Nat. Rev. Immunol.* 6:919–929. doi:10.1038/nri1980

Stow, J.L., P.C. Low, C. Offenhäuser, and D. Sangermani. 2009. Cytokine secretion in macrophages and other cells: pathways and mediators. *Immunobiology.* 214:601–612. doi:10.1016/j.imbio.2008.11.005

Vanhaesebroeck, B., and M.D. Waterfield. 1999. Signaling by distinct classes of phosphoinositide 3-kinases. *Exp. Cell Res.* 253:239–254. doi:10.1006/excr.1999.4701

Vanhaesebroeck, B., M.J. Welham, K. Kotani, R. Stein, P.H. Warne, M.J. Zvelebil, K. Higashi, S. Volinia, J. Downward, and M.D. Waterfield. 1997. P110delta, a novel phosphoinositide 3-kinase in leukocytes. *Proc. Natl. Acad. Sci. USA.* 94:4330–4335. doi:10.1073/pnas.94.9.4330

Vanhaesebroeck, B., S.J. Leevers, K. Ahmadi, J. Timms, R. Katso, P.C. Driscoll, R. Woscholski, P.J. Parker, and M.D. Waterfield. 2001. Synthesis and function of 3-phosphorylated inositol lipids. *Annu. Rev. Biochem.* 70:535–602. doi:10.1146/annurev.biochem.70.1.535

Vanhaesebroeck, B., K. Ali, A. Bilancio, B. Geering, and L.C. Foukas. 2005. Signalling by PI3K isoforms: insights from gene-targeted mice. *Trends Biochem. Sci.* 30:194–204. doi:10.1016/j.tibs.2005.02.008

Wylie, F., K. Heimann, T.L. Le, D. Brown, G. Rabnott, and J.L. Stow. 1999. GAIP, a Galphai-3-binding protein, is associated with Golgi-derived vesicles and protein trafficking. *Am. J. Physiol.* 276:C497–C506.

Wylie, F.G., J.G. Lock, L. Jamriska, T. Khromykh, D.L. Brown, and J.L. Stow. 2003. GAIP participates in budding of membrane carriers at the trans-Golgi network. *Traffic.* 4:175–189.

Yang, Z., H. Li, Z. Chai, M.J. Fullerton, Y. Cao, B.H. Toh, J.W. Funder, and J.P. Liu. 2001. Dynamin II regulates hormone secretion in neuroendocrine cells. *J. Biol. Chem.* 276:4251–4260. doi:10.1074/jbc.M006371200

Yang, J.S., S.Y. Lee, S. Spanò, H. Gad, L. Zhang, Z. Nie, M. Bonazzi, D. Corda, A. Luini, and V.W. Hsu. 2005. A role for BARS at the fission step of COPI vesicle formation from Golgi membrane. *EMBO J.* 24:4133–4143. doi:10.1038/sj.emboj.7600873

Yang, J.S., H. Gad, S.Y. Lee, A. Mironov, L. Zhang, G.V. Beznoussenko, C. Valente, G. Turacchio, A.N. Bonsra, G. Du, et al. 2008. A role for phosphatidic acid in COPI vesicle fission yields insights into Golgi maintenance. *Nat. Cell Biol.* 10:1146–1153. doi:10.1038/ncb1774